Quantitative Roughness Characterization of Non-Gaussian Random Rough Surfaces by Ultrasonic Method Using Pitch-Catch and Pulse-Echo Configurations

M. N. F. Saniman[1*], K. A. A. Wahid[1], F. M. Foudzi[2], H. H. Ladin[3] and I. Ihara[4]
[1]Mechanical Engineering Section, Universiti Kuala Lumpur Malaysia France Institute, 43650 Bangi, Selangor, Malaysia.
[*]Email: mnfarhan@unikl.edu.my
[2]Mechanical Engineering Programme, Faculty of Engineering and Built Environment, Universiti Kebangsaan Malaysia, 43650, Bangi, Selangor, Malaysia.
[3]Department of Mechanical Engineering, Kulliyyah of Engineering, International Islamic University Malaysia, 53100, Gombak, Selangor, Malaysia.
[4]Department of Mechanical Engineering, Faculty of Engineering, Nagaoka University of Technology, 9402188, Nagaoka, Niigata, Japan.

***Abstract*— Fundamental study to quantitatively evaluate not only the root-mean-square (rms) roughness *Rq* but also skewness *Rsk* of non-Gaussian random rough surfaces by ultrasonic method is presented. In this work, Johnson distribution together with Kirchhoff theory have been employed to derive a newly proposed Johnson characteristic function, which provides a theoretical relationship among ultrasonic reflection coefficient, *Rq* and *Rsk*. Based on the characteristics of such relationship, an effective ultrasonic measurement method consisting of a pitch-catch and a pulse-echo configuration to quantitatively characterize *Rq* and *Rsk* has been proposed. A general guideline for such characterization method has also been suggested. The validation of the proposed method has then been conducted numerically in the case of an air-coupled ultrasound. Good agreements between the numerically estimated *Rq* and *Rsk* and the corresponding reference values thus confirm the validity of the proposed method.**

***Index Term*— Johnson characteristic function, Kirchhoff theory, non-Gaussian, skewness, surface roughness, ultrasonic.**

I. Introduction

For many years, surface roughness has been used as an indicator either to control the manufacturing processes or to optimize the engineering functionality of material surfaces [1]. The measurement of such surface roughness is usually conducted post-manufacturing or off-line by using a mechanical stylus profiler [2], which will decrease the production efficiencies and cost effectiveness. Furthermore, such conventional method directly touches the measured surface and caused unnecessary damages [3]. In order to overcome such problems, alternative non-contact methods that are suitable for real-time and on-line roughness characterizations are greatly desired. Among them, ultrasonic method has been proposed as one of the solutions [4-9].

Owing to its fast response time as well as the suitability to be used in an on-line monitoring process, ultrasonic method is considered as a promising method for an automated roughness characterization, especially by an air-coupled ultrasound. Due to a longer wavelength of ultrasonic waves compared to that of electromagnetic waves in an optical method, ultrasonic method is a better choice for a fast roughness characterization involving macro-topography with large profiling area, such as the characterizations of wood lamella [10] and grinding wheel [11] by an air-coupled ultrasound. Moreover, since the optical method in some cases is very sensitive to the existence of dust particles, ultrasonic method is much preferable to overcome such issue. Even though such ultrasonic method has been utilized to estimate the roughness of many material surfaces based on the measured reflection coefficient of ultrasonic waves [4-6, 12], such applications are limited only to rough surfaces having a Gaussian height probability density function (PDF).

However, recent studies reveal that the skewness of non-Gaussian properties for rough surfaces has a strong influence to the tribological behaviours of the surfaces such as lubrication properties [13-15], contact fatigue life [16], and friction coefficient [17, 18]. Furthermore, common machining processes also produce non-Gaussian rough surfaces [19]. For example, honing, grinding, and milling tend to produce surfaces with negative skewness. Despite the existence of such non-Gaussian rough surfaces, many studies that are related to the surface topography of material, including the study of wave scattering from random rough surfaces, assume that a height PDF is Gaussian. Such assumption is generally accepted because it could provide a simple analytical solution and simply because the nature of the examined surface is limited to Gaussian only. However, in some cases, the existence of the non-Gaussian rough surfaces as well as the influences of its properties must be taken into consideration, which lead to the rejection of the Gaussian assumption. Therefore, the quantitative characterization of such non-Gaussian surface roughness is particularly important and the development of a new ultrasonic method to achieve such purpose is greatly desired. To the author's knowledge, such ultrasonic method has never been developed before.

Furthermore, in the ultrasonic method, generally, only the reflection coefficient can be obtained when a rough surface is insonified with ultrasonic waves. Since it is known that the topographic roughness of material surfaces affects the reflection coefficient, it is particularly important to study and understand how the non-Gaussian properties could affect the scattering phenomena of ultrasonic waves. Even though Kirchhoff approximation [20] is one of the most commonly employed waves scattering models, such model mainly addresses the wave scattering from the Gaussian surfaces only [21, 22]. Unfortunately, little is known about the effects of skewness to the reflection coefficient of ultrasonic waves from the non-Gaussian surfaces. In addition, correlations between such statistical parameter and ultrasonic reflection coefficient have not been clearly defined. Consequently, the applications of ultrasonic method to the skewness characterization of non-Gaussian surface roughness have never been studied before, theoretically or experimentally.

The aim of the present study is to quantitatively characterize not only the root-mean-square (rms) roughness *Rq*, but also skewness *Rsk* of the non-Gaussian surfaces by the ultrasonic method. To do so, the theoretical relationship among the reflection coefficient, *Rq*, and *Rsk* at various angles and frequencies has been derived according to the Kirchhoff theory in conjunction with Johnson distribution. The characteristics of such relationships are then examined to investigate the influence of *Rsk* to the ultrasonic reflection coefficient. Based on such investigation results, an effective ultrasonic measurement method to quantitatively characterize the *Rq* and *Rsk* has been proposed. In order to confirm the validity of the proposed method, numerical works in the case of an air-coupled ultrasound have been conducted. The numerically estimated values of *Rq* and *Rsk* are then compared with the reference ones. The agreement between both values, which indicates the validity of the proposed ultrasonic method, is discussed.

II. THEORIES

A. Skewness and Kurtosis

Two main statistical parameters related to the non-Gaussian properties of the height PDF $p(h)$ are skewness *Rsk* and kurtosis *Rku*. *Rsk* is the measure of symmetry while *Rku* is the measure of sharpness of the distribution, which are given by [23]:

$$Rsk = \frac{1}{NRq^3}\sum_{i=1}^{N}(h_i - h^*)^3 p(h_i), \tag{1}$$

$$Rku = \frac{1}{NRq^4}\sum_{i=1}^{N}(h_i - h^*)^4 p(h_i), \tag{2}$$

respectively. Here, N is the samples number, h^* is the mean height, and h is the height. A Gaussian height PDF has a symmetrical shape such that $Rsk = 0$ and $Rku = 3$, whereas a non-Gaussian height PDF is the opposite. A positive *Rsk* ($Rsk > 0$) means that a surface profile has a lot of high peaks while a negative *Rsk* ($Rsk < 0$) means that a surface profile has a lot of deep valleys. On the other hand, $Rku > 3$ represents a surface profile that is concentrated around the mean height while $Rku < 3$ represents a gently undulating surface profile. Common machining processes often produce non-Gaussian finish surfaces with *Rsk* and *Rku* in the range of -1 to 1 and 2 to 10, respectively.

B. Johnson Distribution

For a non-Gaussian surface profile that has an asymmetry or skewed height PDF, it can be described by the unbounded type of Johnson distribution $p(h)_J$, which is given by [24]:

$$p(h)_J = \frac{\delta}{\eta\sqrt{2\pi\left[\left(\frac{h-\xi}{\eta}\right)^2+1\right]}} \times \exp\left(-\frac{1}{2}\left\{\gamma + \delta\ln\left[\frac{h-\xi}{\eta} + \sqrt{\left(\frac{h-\xi}{\eta}\right)^2+1}\right]^2\right\}\right) \tag{3}$$

for $+\infty \le h \le -\infty$. Here, γ, δ, η, and ξ are known as the Johnson parameters, which can be estimated from h^*, *Rq*, *Rsk*, and *Rku* by using Tuenter's algorithm [25]. These four parameters allow the Johnson distribution to be very flexible in describing any shape of a unimodal height PDF. It is noted that *Rsk* and *Rku* must satisfy the following condition [24]:

$$Rku > 1.89Rsk^2 + 3. \tag{4}$$

In this study, focus is given on studying only the effect of *Rq* and *Rsk* to the ultrasonic reflection coefficient, such that the values of h^* is always 0 and *Rku* are related or coupled to *Rsk* by [26]:

$$Rku = 1.89Rsk^2 + 1.65Rsk + 3, \tag{5}$$

so that Eq. (4) is satisfied. Eq. (5) is an optimum relationship to represent the non-Gaussian surfaces in the ultrasonic study. In fact, such increment in *Rku* with *Rsk* is the common properties of engineering surfaces produced by many machining processes such as honing, grinding, and milling [15, 17]. The variations in the height PDFs having $Rq = 75$ μm for various *Rsk* is shown in Fig. 1.

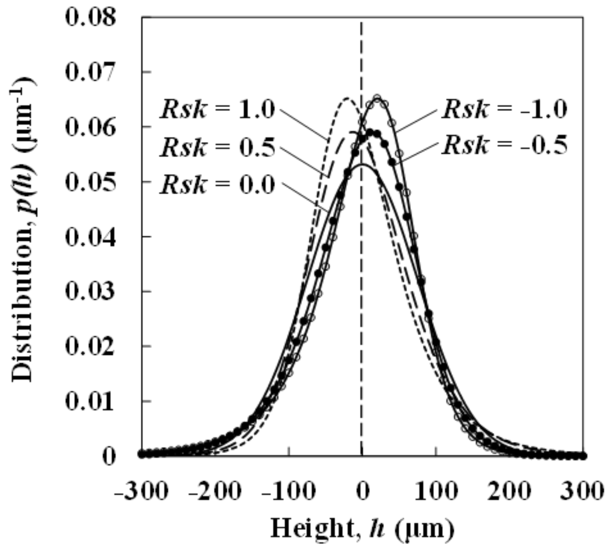

Fig. 1. Height PDF for various *Rsk* values.

C. Kirchhoff Characteristic Function (CF)

Ultrasonic roughness measurement method utilizes the Kirchhoff theory of wave scattering to estimate the statistical parameters of a random rough surface. In such Kirchhoff theory, for a monochromatic plane wave that incidents to a random rough surface at angle θ_1 and then reflected back at angle θ_2, the coherent component of the ultrasonic reflection coefficient I at a distance r from the surface is given by [20]:

$$I = \frac{A_{sc}(r)}{A_0(r)} = \int_{-\infty}^{\infty} \exp\left[-ikh\left(\cos\theta_1 + \cos\theta_2\right)\right] p(h)dh \tag{6}$$

where $k = 2\pi/\lambda = 2\pi f/v$ is the wavenumber, λ is wavelength, f is frequency, v is sound velocity, and A_{sc} and A_0 are the scattered field from a rough and a reference surface, respectively. Moreover, Eq. (6) is known as the Kirchhoff characteristic function (CF) of a rough surface, which is a kind of a Fourier transformation of the height PDF.

III. ULTRASONIC METHOD TO CHARACTERIZE NON-GAUSSIAN SURFACES

A. Theoretical Relationship among Reflection Coefficient I, Rq, and Rsk

By assuming that the random rough surface is having a Gaussian height PDF, based on the Kirchhoff theory, the relationship between the reflection coefficient I and Rq can be expressed in a simple analytical solution, which is given by [27]:

$$I = \exp\left[-\frac{1}{2}k^2 Rq^2\left(\cos\theta_1 + \cos\theta_2\right)^2\right] \tag{7}$$

Such solution has been derived by introducing a Gaussian distribution $p(h)_G$, which is given by:

$$p(h)_G = \frac{1}{Rq\sqrt{2\pi}}\exp\left[-\frac{\left(h-h^*\right)^2}{2Rq^2}\right] \tag{8}$$

into the Kirchhoff CF in Eq. (6). Thus, Eq. (7) is called as the Gaussian CF, which provides the theoretical relationship between I and Rq for a Gaussian surface. Such relationship makes the Rq characterization of a Gaussian random rough surface by ultrasonic method possible. Since Eq. (7) has been derived based on the Gaussian assumption, it means that Rq of a non-Gaussian rough surface cannot be evaluated from I by using the Gaussian CF in Eq. (7). In fact, it has been proven that the use of such Gaussian CF to the characterization of the non-Gaussian surface roughness will lead to an inaccurate Rq estimation by the ultrasonic method [26].

In order to overcome the above-mentioned issue, we proposed that the Johnson distribution $p(h)_J$ given by Eq. (3) to be introduced into the Kirchhoff CF in Eq. (6) as a substitution to the Gaussian distribution $p(h)_G$. As a result, a new CF, which is called Johnson CF, has been obtained, which is given by:

$$I = \frac{\delta}{\eta\sqrt{2\pi}}\int_{-\infty}^{\infty}\left\{\frac{1}{\sqrt{\left[\left(\frac{h-\xi}{\eta}\right)^2+1\right]}}\times\exp\left[-ikh\left(\cos\theta_1+\cos\theta_2\right)\right]\times\exp\left(-\frac{1}{2}\left\{\gamma+\delta\ln\left[\frac{h-\xi}{\eta}+\sqrt{\left(\frac{h-\xi}{\eta}\right)^2+1}\right]^2\right\}\right)\right\}dh \tag{9}$$

However, due to the mathematical complexities, there is no simple analytical solution to Eq. (9) and it must be solved numerically. Nevertheless, the Johnson CF could provide the theoretical relationship among I, Rq, and Rsk at various angles θ and frequencies f, where such relationship has never been derived before.

For given values of $Rq = 0 \sim 500$ μm and $Rsk = -1 \sim 1$, the theoretical relationship among the values of I, Rq, and Rsk which were calculated according to Eq. (9) are shown in Fig. 2. Note that a normalized form of Rq, $Rq \cdot \cos\theta/\lambda$, is being used in the x-axis. Such normalization provides a generalization to the changes of I with Rq for various Rsk regardless of specular angle θ ($\theta = \theta_1 = \theta_2$) and wavelength λ. In addition, the absolute value of Rsk, $|Rsk|$, are being used because both positive and negative Rsk values show an identical trend.

In general, it is shown in Fig. 2 that I decreases exponentially

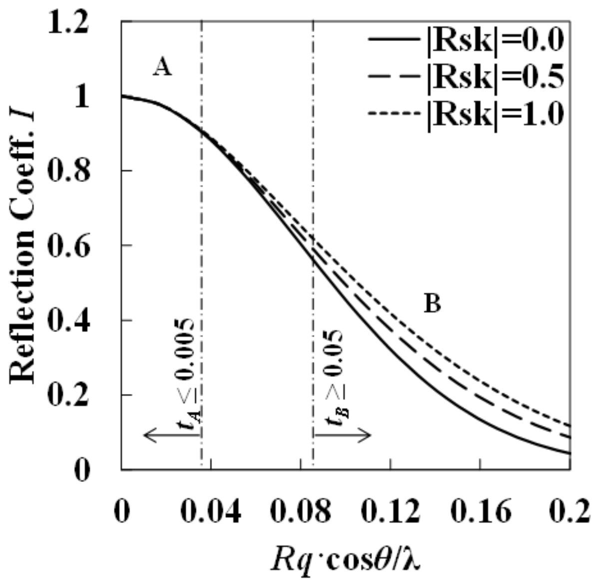

Fig. 2. Changes of *I* with normalized *Rq* for various *Rsk* values.

as normalized *Rq* increases. Interestingly, it is found that *I* of each |*Rsk*| changes differently depending on the values of normalized *Rq*, *Rq*·cos*θ*/*λ*. At a relatively small *Rq*·cos*θ*/*λ* value (region A), regardless of |*Rsk*|, there is almost no discrepancy in the values of *I*, which indicates that the influence of |*Rsk*| to *I* is negligible at such range of roughness. On the other hand, at a relatively large *Rq*·cos*θ*/*λ* value (region B), the influence of |*Rsk*| to the changes of *I* is significant and no longer negligible. These two contradict characteristics of *I* at small and large *Rq*·cos*θ*/*λ* could be useful to develop a new quantitative ultrasonic method for the characterization of *Rq* and |*Rsk*| of the non-Gaussian rough surfaces.

B. *Quantitative Characterization of Rq and Rsk*

To quantitatively define the region *A* and *B* mentioned above, a threshold value *t* is proposed, which is given by:

$$t = I_{|Rsk|=1} - I_{|Rsk|=0} \qquad (10)$$

where *t* is the difference of *I* when |*Rsk*| = 0 and |*Rsk*| = 1. $t_A \leq 0.005$ is defined as region A while $t_B \geq 0.05$ is defined as region *B*, where $t_B = 10t_A$. The values of *Rq*·cos*θ*/*λ* when $t_A = 0.005$ and $t_B = 0.05$ are 0.037 and 0.081, respectively, as shown in Fig. 2. It should be noted that the value of *t* could be changed to any desired values depending on the purpose of the measurement and accuracy of the equipment used.

Furthermore, in the region *A* where the influence of *Rsk* to *I* is negligible, the changes of *I* with *Rq* can be represented by the Gaussian CF in Eq. (7). This means that the *Rq* of a non-Gaussian rough surface can be estimated from the value of *I* regardless of *Rsk*. On the other hand, in the region B where the influence of *Rsk* to *I* is significant, the *Rsk* of the non-Gaussian surface can be estimated based on the Johnson CF in Eq. (9) from the value of *I* when *Rq* value is known. Thus, the quantitative characterizations of *Rq* and *Rsk* of the non-Gaussian surfaces can be done by firstly determining the value of *Rq* in the region *A* where *Rq*·cos*θ*/*λ* is small and then using it to determine *Rsk* in the region *B* where *Rq*·cos*θ*/*λ* is large.

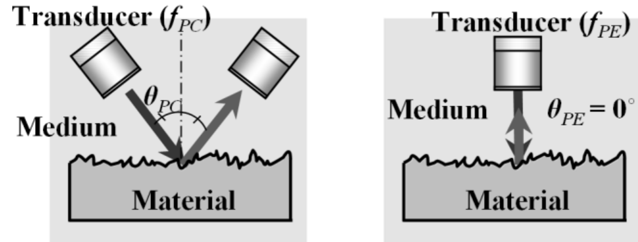

Fig. 3. Schematic diagram of (a) pitch-catch and (b) pulse-echo configurations of the ultrasonic measurement method.

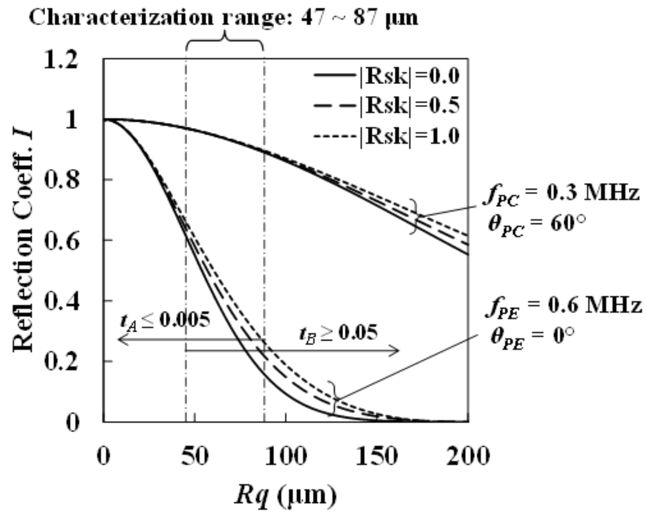

Fig. 4. Changes of *I* with *Rq* for various *Rsk* at PC (*f* = 0.3 MHz and *θ* = 60°) and PE (*f* = 0.6 MHz and *θ* = 0°) configurations in the air (*v* = 345 m/s).

The value of *Rq*·cos*θ*/*λ* depends on its normalization factors, which are the specular angle *θ* and wavelength *λ*. Since *λ*=*v*/*f*, *f* becomes the variable parameter to define *λ* when *v* is constant. To obtain a relatively small *Rq*·cos*θ*/*λ* value that is needed to characterize *Rq*, a small *f* and a large *θ* are the best combination. On the other hand, to obtain a relatively large *Rq*·cos*θ*/*λ* value that is needed to characterize *Rsk*, a large *f* and a small *θ* are the best combination. In practical ultrasonic measurements, these two different combinations of *f* and *θ* can be realized by using a pitch-catch (PC) and a pulse-echo (PE) configuration, as shown in Fig. 3. In the PC configuration, *θ* must be large enough to ensure the *Rq* characterization is possible while in the PE configuration, *θ* = 0°, which is the smallest possible value. Thus, a new ultrasonic measurement method which combines both PC and PE configurations is proposed to quantitatively characterize *Rq* and *Rsk* of a non-Gaussian surface.

To understand further about the proposed ultrasonic method, roughness measurements by an air-coupled ultrasound are used as an example. Fig. 4 shows the theoretical relationship among

I, *Rq*, and *Rsk* for ultrasonic waves that propagate in air (v = 345 m/s) at two different combinations of f and θ. In the PC configuration, f_{PC} = 0.3 MHz and θ_{PC} = 60° while in the PE configuration, f_{PE} = 0.6 MHz and θ_{PE} = 0°. Such values of f and θ are considered as the commonly used values in the air-coupled ultrasonic method. It can be seen in Fig. 4 that $t_A \leq 0.005$ occurs when $Rq \leq 87$ µm, where such range is useful to characterize *Rq*, while $t_B \geq 0.05$ occurs when $Rq \geq 47$ µm, where such range is useful to characterize *Rsk*. The overlapping region of t_A and t_B, which lies in the range of 47 µm ≤ *Rq* ≤ 87 µm, represents the range of *Rq* where *Rsk* can be characterized quantitatively by the proposed method. Thus, depending on the selected combinations of f and θ, there is a limitation to the range of *Rq* where the proposed method is applicable. On the other hand, if the measurable range of *Rq* has been fixed, the appropriate combinations of f and θ must be used. Most importantly, the proposed characterization method is not only applicable for the noncontact ultrasonic method such as air-coupled and water immersion technique, but also the contact ultrasonic methods for the characterization of *Rq* and *Rsk* of the back surface or interface of materials.

Moreover, a general guideline is proposed in order to quantitatively characterize the *Rq* and *Rsk* of a non-Gaussian rough surface, which is given by the following steps:

1. Define the values of f_{PC} and θ_{PC} of the pitch-catch configuration.
2. Measure the value of I_{PC} of the rough surface at f_{PC} and θ_{PC}.
3. Estimate Rq_{PC} from I_{PC} based on the Gaussian CF.
4. Define the values of f_{PE} of the pulse-echo configuration ($\theta_{\mathrm{PE}} = 0°$).
5. Measure the value of I_{PE} of the rough surface at f_{PE} and θ_{PE}.
6. Using the estimated Rq_{PC} value in Step 3 and the values of f_{PE} and θ_{PE} in Step 4, calculate the theoretical relationship between *I* and *Rsk* based on the Johnson CF and then determine the fitted equation using a least-square method.
7. Estimate Rsk_{PE} from I_{PE} based on the fitted equation in Step 6.

In order to verify the validity of the proposed characterization method, a numerical approach has been used due to the difficulties in fabricating the non-Gaussian specimens having the desired and exact values of *Rq* and *Rsk*. In fact, similar approach has been used extensively to study the tribological properties of the non-Gaussian surfaces [28-30].

IV. NUMERICAL VALIDATIONS

A. Generation of Non-Gaussian Random Rough Surfaces

Following the theoretical works in the previous section, numerical validations for the proposed ultrasonic method are conducted in the case of an air-coupled ultrasonic method. In such validations, a series of non-Gaussian random rough surfaces having the desired Johnson height PDF has been simulated numerically. To do so, a method based on Fourier transformations proposed by Wu [31] has been used. Each surface is set to a length (x) of 20 mm and spatial length (dx) of 0.02 mm. Such surfaces are designed to have predefined values of *Rq* and *Rsk*, which is given by Table I. It can be seen that the range of *Rq* and *Rsk* are 50 to 85 µm and -1 to 1, respectively, which lies in the possible characterization range of *Rq* and *Rsk* by air-coupled ultrasound as shown in Fig. 4. Moreover, for each combination values of *Rq* and *Rsk*, 50 independent surfaces have been simulated. Fig. 5 shows examples of the simulated surfaces and their corresponding height PDFs having *Rsk* = 0.0, 1.0, and -1.0. The existence of high peaks and deep valleys can be observed in Fig. 5b and Fig. 5c, respectively, where it is a common surface feature of a skewed surface profile. Note that in the present study, a smooth Gaussian surface with *Rq* = 0.01 µm has been used as the reference surface.

Table I
Properties of the generated surface profiles.

Profile	*Rq* (µm)	*Rsk*
1	50	0.0
2	50	0.8
3	55	-0.3
4	60	0.5
5	60	-0.8
6	65	0.3
7	70	-0.5
8	70	1.0
9	75	-0.7
10	80	0.0
11	80	-1.0
12	85	0.7

B. Reflection Coefficient Estimation

For each of the simulated non-Gaussian surfaces where the values of height deviation from the mean height dh are known, the coherent ultrasonic reflection coefficient I^* can easily be determined by [32]:

$$I^* = \int_{-\infty}^{\infty} \left(\sin\theta_1 \frac{dh}{dx} + \cos\theta_1 \right) \times \exp\left[ik\left\{ \left(\sin\theta_1 - \sin\theta_2\right)x - \left(\cos\theta_1 + \cos\theta_2\right)dh \right\} \right] dx \tag{11}$$

which is the general solution for wave scattering problem from a random rough surface having any kind of height PDF, including the non-Gaussian ones. Using Eq. (11), I_{PC} has been determined at f_{PC} = 0.3 MHz and $\theta_{PC} = \theta_1 = \theta_2 = 60°$ while I_{PE} at f_{PE} = 0.6 MHz and $\theta_{PE} = \theta_1 = \theta_2 = 0°$, which are the same values used in the theoretical work's example in the previous section. The averaged values of I_{PC} and I_{PE} over 50 independently generated surfaces for each combination of *Rq* and *Rsk* shown in Table I are used in the discussions.

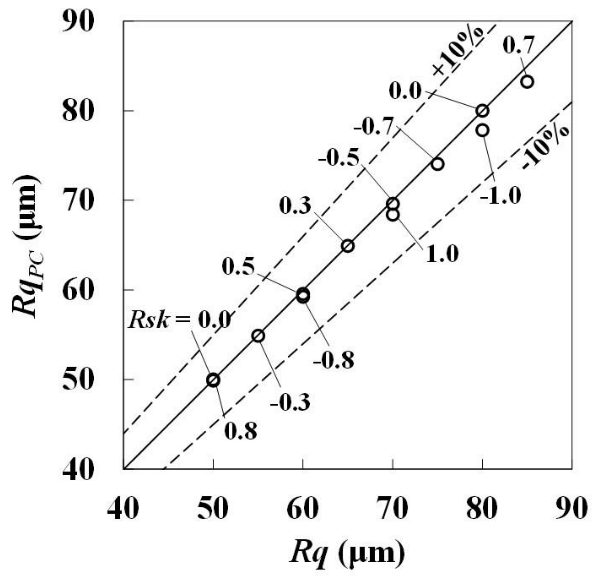

Fig. 7. Comparison between the numerically estimated Rq_{PC} and theoretical Rq.

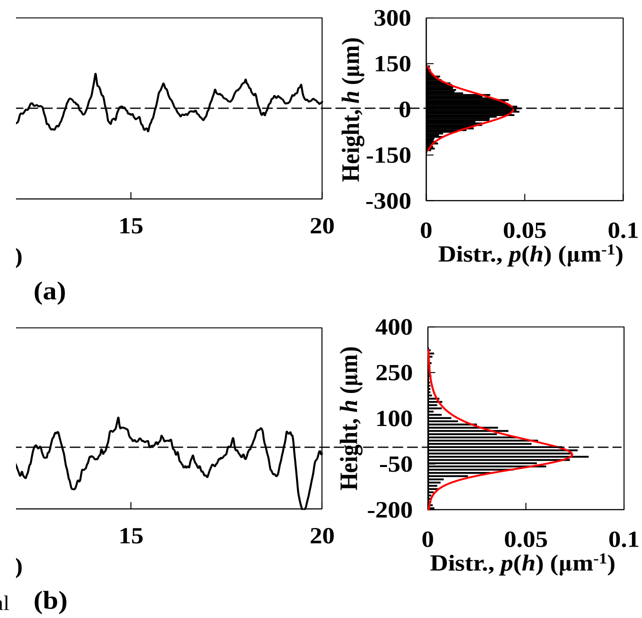

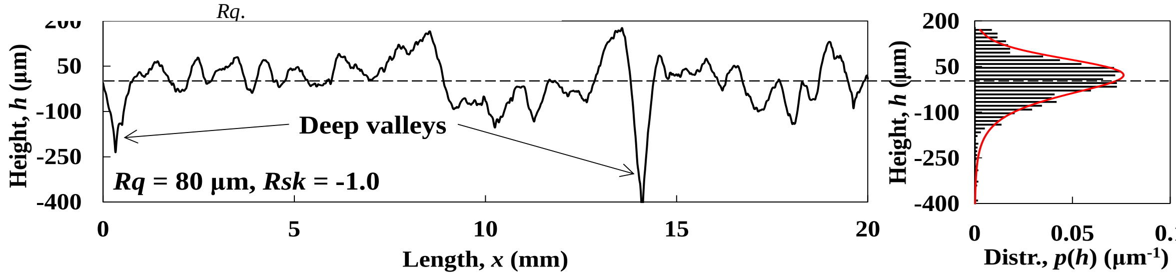

(c)

Fig. 5. Simulated non-Gaussian rough surfaces and its corresponding height PDFs having (a) Rsk = 0.0, (b) Rsk = 1.0, and (c) Rsk = -1.0.

V. RESULTS AND DISCUSSIONS

In order to confirm the validity of the proposed method, Rq and Rsk of the simulated surfaces are going to be estimated from the averaged values of I_{PC} and I_{PE} based on the proposed guideline. Following the guideline, it is noted that Steps 1, 2, 4,

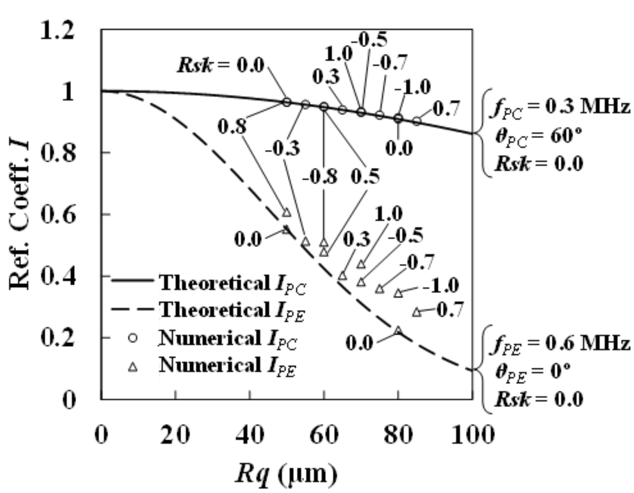

Fig. 6. Changes of the theoretical and numerical reflection coefficients with Rq.

and 5 have been done in the previous section, since these values are predefined. Fig. 6 shows the numerically estimated I_{PC} and I_{PE} of the simulated non-Gaussian surfaces compared to the theoretical values having Rsk = 0 determined at the corresponding values of f and θ. In general, both numerical I_{PC} and I_{PE} decrease as Rq increases. In particular, it is observed that regardless of Rsk, the numerical I_{PC} agree well with the theoretical one having Rsk = 0 (denoted by solid line). Such results thus indicate that the influence of Rsk to I is negligible at the PC configuration. On the other hand, it is observed that the numerical I_{PE} having various Rsk deviate from the theoretical one having Rsk = 0 (denotes by dashed line), which indicate a significant influence of Rsk to I at the PE configuration. Such influence can clearly be observed from the profiles having same Rq but different Rsk, e.g. those with Rq = 80 µm but Rsk = 0 and -1.

Then, based on Step 3 of the guideline, the value of Rq_{PC} have been estimated from the measured I_{PC} using the Gaussian CF that is given by:

$$Rq_{PC} = \sqrt{\ln\left(I_{PC}\right) \Big/ \left[-4\left(\frac{\pi f_{PC}}{v}\right)^2 \cos^2\theta_{PC}\right]} \qquad (12)$$

which has been derived from Eq. (7). Fig. 7 shows the comparison between the numerically estimated Rq_{PC} and the reference ones given in Table I. A very good agreement with ±3% of error is obtained between both values. Such agreement provides evidence that the *Rq* of any non-Gaussian rough surfaces could be accurately evaluated when the value of $Rq \cdot \cos\theta/\lambda$ is relatively small, as shown in Fig. 4, where such small $Rq \cdot \cos\theta/\lambda$ has been obtained through the PC configuration. It has been mentioned before that at such range of $Rq \cdot \cos\theta/\lambda$, the influence of *Rsk* to *I* could be neglected which make the *Rq* estimation is possible. The estimated Rq_{PC} is then used to quantitatively evaluate *Rsk*.

Following Step 6 of the guideline, for each of the estimated Rq_{PC} in Fig. 7, the theoretical relationship between *I* and *Rsk* at PE configuration have been obtained based on the Johnson CF given by Eq. (9). Fig. 8 shows such changes of *I* with *Rsk* for each Rq_{PC} and the corresponding fitted equations are summarized in Table II.

Finally, following Step 7 of the guideline, the values of Rsk_{PE} have been estimated from the values of I_{PE} shown in Fig. 6 by using the fitted equations given in Table II. Fig. 9 shows the comparison between the numerically estimated Rsk_{PE} and its reference values given in Table I. A good agreement with approximately +20% of error is obtained between both values. Such result indicates that the *Rsk* of any non-Gaussian rough surfaces could be quantitatively evaluated when *Rq* is known (through the ultrasonic measurement at PC configuration) and the value of $Rq \cdot \cos\theta/\lambda$ is relatively large, as shown is Fig. 4. Here, such large $Rq \cdot \cos\theta/\lambda$ value has been obtained through the PE configuration. It is important to note here that the estimation error of Rq_{PC} is included in the estimation error of Rsk_{PE} due to the fact that Rq_{PC} has been used in estimating Rsk_{PE}. This means that a large error in Rq_{PC} estimation will lead to a large error in Rsk_{PE} estimation. Moreover, as shown in Fig. 8, the dynamic range of the changes of *I* with *Rsk* is small, which indicates that a slight deviation in I_{PE} from its ideal value will cause a large error in the estimated Rsk_{PE}. Therefore, precise measurements of I_{PC} and I_{PE} are needed in order to accurately evaluate *Rq* and *Rsk* using the proposed method. In overall, the consistencies between the estimated Rq_{PC} and Rsk_{PE} compared to the reference values indicate that the validity of the proposed ultrasonic method in quantitative characterization of the non-Gaussian rough surfaces has been confirmed.

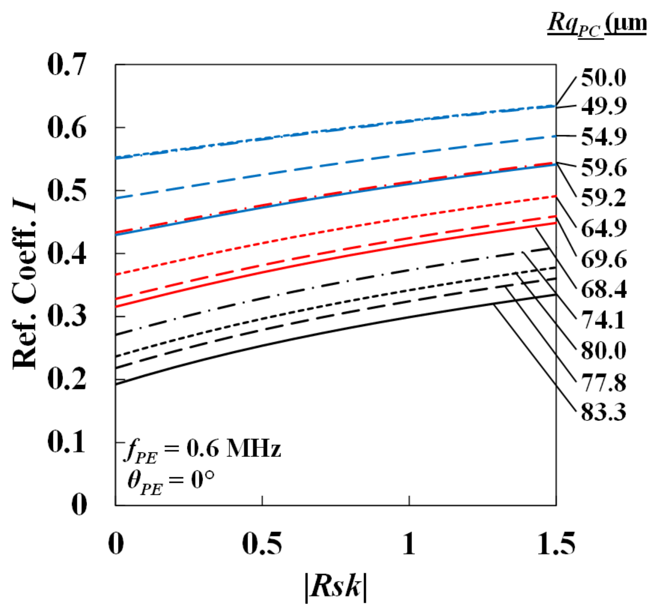

Fig. 8. Changes of *I* with *Rsk* for various Rq_{PC}.

Table II
Fitted equations of the relationship between *I* and *Rsk* for each Rq_{PC}.

Pro-file	Rq_{PC} (µm)	Fitted Equations
1	50.0	$I_{PE} = -0.0067\lvert Rsk\rvert^2 + 0.0660\lvert Rsk\rvert + 0.5500$
2	49.9	$I_{PE} = -0.0066\lvert Rsk\rvert^2 + 0.0657\lvert Rsk\rvert + 0.5516$
3	54.9	$I_{PE} = -0.0093\lvert Rsk\rvert^2 + 0.0801\lvert Rsk\rvert + 0.4873$
4	59.6	$I_{PE} = -0.0118\lvert Rsk\rvert^2 + 0.0926\lvert Rsk\rvert + 0.4294$
5	59.2	$I_{PE} = -0.0116\lvert Rsk\rvert^2 + 0.0918\lvert Rsk\rvert + 0.4333$
6	64.9	$I_{PE} = -0.0145\lvert Rsk\rvert^2 + 0.1049\lvert Rsk\rvert + 0.3671$
7	69.6	$I_{PE} = -0.0166\lvert Rsk\rvert^2 + 0.1133\lvert Rsk\rvert + 0.3168$
8	68.4	$I_{PE} = -0.0161\lvert Rsk\rvert^2 + 0.1114\lvert Rsk\rvert + 0.3291$
9	74.1	$I_{PE} = -0.0181\lvert Rsk\rvert^2 + 0.1191\lvert Rsk\rvert + 0.2728$
10	80.0	$I_{PE} = -0.0195\lvert Rsk\rvert^2 + 0.1233\lvert Rsk\rvert + 0.2207$
11	77.8	$I_{PE} = -0.0191\lvert Rsk\rvert^2 + 0.1222\lvert Rsk\rvert + 0.2388$
12	83.3	$I_{PE} = -0.0200\lvert Rsk\rvert^2 + 0.1239\lvert Rsk\rvert + 0.1953$

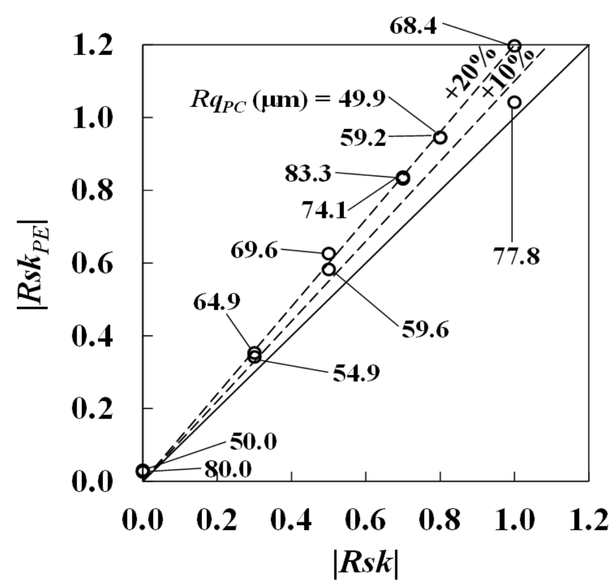

Fig. 9. Comparison between the numerically estimated Rsk_{PE} and theoretical *Rsk*

VI. Conclusion

An effective method for quantitative characterization of *Rq* and *Rsk* of the non-Gaussian rough surfaces by ultrasound has been presented. In this study, to conduct such characterizations, a generalized relationship among the ultrasonic reflection coefficient *I*, *Rq*, and *Rsk* has been obtained from a newly derived Johnson characteristic function. It has been found that the influence of *Rsk* to *I* is negligible at relatively small normalized *Rq* (e.g. $Rq \cdot \cos\theta/\lambda \leq 0.037$) and is significant at relatively large normalized *Rq* (e.g. $Rq \cdot \cos\theta/\lambda \geq 0.081$). Such characteristics of *Rsk* to *I* have been used as the basis to develop an effective ultrasonic measurement method that combines the pitch-catch and pulse-echo configurations to quantitatively characterize *Rq* and *Rsk*. Then, the validity of the proposed method has been verified numerically in the case of an air-coupled ultrasound, where it has been found that the numerically estimated *Rq* and *Rsk* are consistent with that of reference values. Based on the present study, the feasibility of the application of the proposed ultrasonic method in practical measurements will be conducted in the future through a series of experimental measurements.

ACKNOWLEDGMENT

Financial support through Grants-in-Aid for Scientific Research (B25289238) from the Japan Society for the Promotion of Science is greatly appreciated. Technical support from Universiti Kuala Lumpur Malaysia France Institute is also appreciated.

REFERENCES

[1] D. J. Whitehouse, *Handbook of Surface and Nanometrology*, 2nd ed. Boca Raton: CRC Press, 2010.

[2] T. R. Thomas, *Rough Surfaces*, 2nd ed. London: Imperial College Press, 1999, p. 278.

[3] P. Sutowski, K. Nadolny, M. Ungureanu, and W. Kapłonek, "Stylus Profilometry in Surface Roughness Measurements of the Vertical Conical Mixing Unit Used in a Food Industry," *Journal of Mechanical Engineering*, vol. 47, no. 1, pp. 1-8, 2018, doi: 10.3329/jme.v47i1.35352.

[4] D. D. Sukmana and I. Ihara, "Application of Air-Coupled Ultrasound to Noncontact Surface Roughness Evaluation," *Japanese Journal of Applied Physics*, vol. 44, no. 6B, pp. 4417-4420, 2005, doi: 10.1143/jjap.44.4417.

[5] D. D. Sukmana and I. Ihara, "Surface Roughness Characterization through the Use of Diffuse Component of Scattered Air-Coupled Ultrasound," *Japanese Journal of Applied Physics*, vol. 45, no. 5B, pp. 4534-4540, 2006, doi: 10.1143/jjap.45.4534.

[6] D. D. Sukmana and I. Ihara, "Quantitative Evaluation of Two Kinds of Surface Roughness Parameters Using Air-Coupled Ultrasound," *Japanese Journal of Applied Physics*, vol. 46, no. 7B, pp. 4508-4513, 2007, doi: 10.1143/jjap.46.4508.

[7] Y. Fang, L. Lin, H. Feng, Z. Lu, and G. W. Emms, "Review of the use of air-coupled ultrasonic technologies for nondestructive testing of wood and wood products," *Computers and Electronics in Agriculture*, vol. 137, pp. 79-87, 2017, doi: 10.1016/j.compag.2017.03.015.

[8] M. Lian, H. Liu, L. Zhou, T. Zhang, B. Liu, and Y. Wang, "Ultrasonic roughness measurement based on scattering attenuation," *Surface Topography: Metrology and Properties*, vol. 7, no. 1, 2019, doi: 10.1088/2051-672X/aafa4f.

[9] T. Kamigaki, K. Nakatsuma, Y. Oshima, and I. Torigoe, "Detection of ultrasound pressure distribution for remote measurement of haptic surface roughness," presented at the 2015 Ieee Sensors, 2015.

[10] E. Žukauskas, R. Raišutis, A. Voleišis, A. Vladišauskas, and L. Kairiūkštis, "Investigation of the quality of the surface of wood lamellas using air-coupled ultrasonic technique," *Ultragarsas*, vol. 63, no. 3, pp. 33-37, 2008.

[11] N. Arunachalam, R. AnandKumar, and B. Ramamoorthy, "A preliminary investigation on the application of air-coupled ultrasound to evaluate surface condition of the grinding wheel," *International Journal of Abrasive Technology*, vol. 4, no. 3, pp. 266-278, 2011, doi: 10.1504/ijat.2011.042823.

[12] M. N. F. Saniman and I. Ihara, "Application of Air-Coupled Ultrasound to Noncontact Evaluation of Paper Surface Roughness," *Journal of Physics: Conference Series*, vol. 520, p. 012016, 2014, doi: 10.1088/1742-6596/520/1/012016.

[13] N. Yu and A. A. Polycarpou, "Contact of Rough Surfaces With Asymmetric Distribution of Asperity Heights," *Journal of Tribology*, vol. 124, no. 2, 2002, doi: 10.1115/1.1403458.

[14] B. Podgornik, L. M. Vilhena, M. Sedlaček, Z. Rek, and I. Žun, "Effectiveness and design of surface texturing for different lubrication regimes," *Meccanica*, vol. 47, no. 7, pp. 1613-1622, 2012, doi: 10.1007/s11012-012-9540-7.

[15] L. Chang and Y.-R. Jeng, "Effects of negative skewness of surface roughness on the contact and lubrication of nominally flat metallic surfaces," *Proceedings of the Institution of Mechanical Engineers, Part J: Journal of Engineering Tribology*, vol. 227, no. 6, pp. 559-569, 2012, doi: 10.1177/1350650112465365.

[16] X.-L. Yan, X.-L. Wang, and Y.-Y. Zhang, "Influence of Roughness Parameters Skewness and Kurtosis on Fatigue Life Under Mixed Elastohydrodynamic Lubrication Point Contacts," *Journal of Tribology*, vol. 136, no. 3, 2014, doi: 10.1115/1.4027480.

[17] Y. S. Kang, C. H. Hager, and R. D. Evans, "Effects of Skewed Surface Textures on Lubricant Film Thickness and Traction," *Tribology Transactions*, vol. 58, no. 3, pp. 397-406, 2015, doi: 10.1080/10402004.2014.980592.

[18] M. Sedlaček, L. M. S. Vilhena, B. Podgornik, and J. Vižintin, "Surface Topography Modelling for Reduced Friction," *Strojniški vestnik – Journal of Mechanical Engineering*, vol. 57, no. 09, pp. 674-680, 2011, doi: 10.5545/sv-jme.2010.140.

[19] K. J. Stout, "Surface roughness ~ measurement, interpretation and significance of data," *Materials & Design*, vol. 2, no. 5, pp. 260-265, 1981, doi: 10.1016/0261-3069(81)90069-8.

[20] J. A. Ogilvy and H. M. Merklinger, "Theory of Wave Scattering from Random Rough Surfaces," *The Journal of the Acoustical Society of America*, vol. 90, no. 6, pp. 3382-3382, 1991, doi: 10.1121/1.401410.

[21] F. Shi, M. J. S. Lowe, X. Xi, and R. V. Craster, "Diffuse scattered field of elastic waves from randomly rough surfaces using an analytical Kirchhoff theory," *Journal of the Mechanics and Physics of Solids*, vol. 92, pp. 260-277, 2016, doi: 10.1016/j.jmps.2016.04.003.

[22] A. Velichko, L. Bai, and B. W. Drinkwater, "Ultrasonic defect characterization using parametric-manifold mapping," *Proceedings of the Royal Society A: Mathematical, Physical and Engineering Sciences*, vol. 473, no. 2202, 2017, doi: 10.1098/rspa.2017.0056.

[23] E. S. Gadelmawla, M. M. Koura, T. M. A. Maksoud, I. M. Elewa, and H. H. Soliman, "Roughness parameters," *Journal of Materials Processing Technology*, vol. 123, no. 1, pp. 133-145, 2002, doi: 10.1016/s0924-0136(02)00060-2.

[24] N. L. Johnson, "Systems of frequency curves generated by methods of translation," *Biometrika*, vol. 36, no. 1/2, pp. 149-176, 1949.

[25] H. J. H. Tuenter, "An algorithm to determine the parameters ofSU-curves in the johnson system of probabillity distributions by moment matching∗," *Journal of Statistical Computation and Simulation*, vol. 70, no. 4, pp. 325-347, 2001, doi: 10.1080/00949650108812126.

[26] M. N. F. Saniman and I. Ihara, "Feasibility study on characterization of non-Gaussian rough surface by ultrasonic reflection method with the Kirchhoff theory," *Mechanical Engineering Journal*, vol. 3, no. 6, pp. 16-00162, 2016, doi: 10.1299/mej.16-00162.

[27] J. E. Harvey, "Modified Beckmann-Kirchhoff scattering model for rough surfaces with large incident and scattering angles," *Optical Engineering*, vol. 46, no. 7, 2007, doi: 10.1117/1.2752180.

[28] S. Zhang, W. Wang, and Z. Zhao, "The effect of surface roughness characteristics on the elastic–plastic contact performance," *Tribology International*, vol. 79, pp. 59-73, 2014, doi: 10.1016/j.triboint.2014.05.016.

[29] G. Pawar, P. Pawlus, I. Etsion, and B. Raeymaekers, "The Effect of Determining Topography Parameters on Analyzing Elastic Contact Between Isotropic Rough Surfaces," *Journal of Tribology*, vol. 135, no. 1, p. 011401, 2012, doi: 10.1115/1.4007760.

[30] A. Ghosh and F. Sadeghi, "A novel approach to model effects of surface roughness parameters on wear," *Wear*, vol. 338-339, pp. 73-94, 2015, doi: 10.1016/j.wear.2015.04.022.

[31] J.-J. Wu, "Simulation of non-Gaussian surfaces with FFT," *Tribology International*, vol. 37, no. 4, pp. 339-346, 2004, doi: 10.1016/j.triboint.2003.11.005.

[32] J. A. Ogilvy, "Computer simulation of acoustic wave scattering from rough surfaces," *Journal of Physics D: Applied Physics*, vol. 21, no. 2, pp. 260-277, 1988, doi: 10.1088/0022-3727/21/2/006.